Progress In Electromagnetics Research, PIER 102, 1–14, 2010

AN UNBIASED DUAL-MODE MIXING ANTENNA FOR WIRELESS TRANSPONDERS

J. Á. García, L. Cabria, and R. Marante

Department of Communication Engineering
University of Cantabria
39005 Santander, Spain

L. Rizo

Department of Telecommunications
ISPJAE
Ciudad Habana, Cuba

Á. Mediavilla

Department of Communication Engineering
University of Cantabria
39005 Santander, Spain

Abstract—A zero-bias dual-mode mixing antenna for wireless transponders is proposed in this paper. Designed over an Enhancement-mode Pseudomorphic HEMT (E-PHEMT), the mixer takes advantage of the device nonlinear characteristics around cold operation. Simple closed form expressions, obtained from time-varying circuit analysis, predict good conversion efficiency in two different operating modes without requiring DC bias. For validation, a lab prototype has been implemented and tested, to be finally integrated in a compact active printed antenna suitable for wireless sensor networks or other radio frequency identification (RFID) applications.

1. INTRODUCTION

In recent years, a tremendous development of automatic identification systems, and in particular of those non requiring physical contact, has been experienced. That is the case of radio frequency identification techniques (RFID), where transponders [1] are interrogated at a

Corresponding author: L. Cabria (lorena.cabria@unican.es).

distance by a radio frequency or microwave beam that forces them to emit a coded response. Different wireless applications have so emerged, including access control, tall collection or sensor networks among many others.

Simple backscattering techniques with amplitude [2], SSB [3], or other kind of modulation are being employed, with the interference characteristics associated to the use of the same interrogating frequency [4]. Other operating principles try to avoid this inconvenience through the generation of a harmonically related response frequency [5], but may be strongly influenced by undesired reflections of the transmitted harmonics. Designers are not only faced to the false detection problem caused by interference, but also to the efficiency and security limitations imposed by the scarce control these techniques provide over the response radiation direction.

The evolution towards a robust control system necessarily implies the use of frequency translating functions [6], where the response signal appears apart from the interrogating fundamental and harmonic spectral positions. On the other hand, the introduction of a spatially selective radiation capability is dependent on the availability of low cost automatic beamforming solutions. Phase conjugation (retrodirective) arrays [7, 8] stand among the most promising candidates on this line, being also based on the use of heterodyne techniques [9].

The implementation of frequency translating functions as part of RFID technology evolution has been however restrained by the imperious need for minimizing tag DC power consumption (to avoid the use of batteries, or simply to extend their lifetime). That is the reason why FET mixers [10], requiring small LO power levels, offering either conversion gain in active configurations or high linearity in resistive implementations, have still a limited acceptance in the field.

In this paper, a zero-bias dual-mode FET mixing antenna for wireless transponders is proposed. The mixer takes advantage of the nonlinear characteristics of an E-PHEMT around cold operation, being able of reconfiguring between two different operating modes (resistive and active) with good conversion figures. In Section 2, a time-varying circuit analysis of both mixing modes is developed. Extracted closed-form expressions predict optimum conversion conditions when employing an unbiased E-PHEMT. Measured figures for an implemented lab model are also presented, validating the proposed approach. Finally, the mixer is combined with a printed radiator in a time-varying active antenna element. When employed as a single transponder, it is able of sending a coded tag response after being interrogated by a nearby reader. If integrated in an array, it presents the capability of automatically retransmitting a

signal back to a remote interrogator without any priori knowledge of its position.

2. DUAL-MODE E-PHEMT MIXER

FET mixers are usually operated in a region where a maximum change of a first order equivalent circuit parameter, with respect to a control voltage, may be obtained [10]. Such a control voltage determines the port where the local oscillator (LO) signal has to be applied, while the parameter is responsible for the selection of the radio frequency (RF) and intermediate frequency (IF) signal ports.

In a resistive mixer [10], the cold FET output conductance, G_{ds}, dependence on the gate-to-source control voltage, V_{gs}, is employed to create a kind of "linear" time-varying resistance between the drain and source terminals. On the other hand, drain active mixers [10] take advantage of the transconductance, G_m, variation with the drain-to-source voltage, V_{ds}, around the knee of the device I/V characteristic.

Balanced topologies have been proposed for both resistive and active FET mixers, in order to avoid the generation of unwanted spurious components, improve the isolation between ports or reduce the AM LO noise conversion [10]. A good performance could be obtained if the devices were perfectly matched, something difficult to assure in low cost hybrid technologies.

2.1. Single-device Dual-mode Topology

A family of single-device singly-balanced resistive mixers was proposed by Yhland et al. in [11]. A 180° hybrid connection of the drain and source terminals to the RF and IF signal ports was there employed, reducing this way the problems associated with device pairing. Based on that work, the authors proved in [12] the potentiality of a single-device singly-balanced E-PHEMT drain mixer for providing conversion gain at $V_{GS} = V_{DS} = 0\,\mathrm{V}$. A lab model was then constructed and tested, and a 4.17 dB conversion gain was measured at an 8.5 dBm LO power level.

Combining both solutions, a simplified schematic of the here proposed dual-mode mixer is presented in Fig. 1. In the resistive mixing mode, the generator in gate side represents the LO excitation while the other stands for the interrogating signal. In the drain/source mixing mode, however, the generator connected to gate terminal represents the low frequency data signal to be up-converted thanks to a LO pumping component applied between drain and source pads.

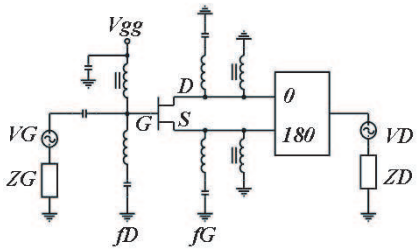

Figure 1. Simplified schematic for the dual-mode singly-balanced topology.

The included resonant circuits provide short-circuit terminations at gate (f_D) and drain/source (f_G) terminals for an optimum mixing performance.

2.2. Resistive Mixing Mode for Phase Conjugated Operation

In this first mode, a LO excitation is used to control gate potential. The interrogating signal, applied in a balanced way to the drain and source terminals, $V_D = V_{int}$, mixes with the time varying output conductance to generate the desired response component. Using a LO at nearly twice the interrogating frequency, $f_{LO} = 2 \cdot f_{int} + \Delta f$, the lower side band mixing component, $f_{resp} = f_{LO} - f_{int}$, would appear close the spectral position of the interrogation, $f_{resp} = f_{int} + \Delta f$. The response would be a phase conjugated version of the interrogation, $\varphi_{resp} = \varphi_{LO} - \varphi_{int}$, required condition for assuring retrodirectivity [7–9]. As considered in [13], the resonant circuits at drain and source terminals guarantee the desired even mode reflection value, $\Gamma e = -1$, at f_{LO}.

According to this operation, a simplified spectral diagram is represented in Fig. 2(a). The mixing frequency positions follow a notation similar to the employed for conversion matrix analysis in [14], $f_n = |n \cdot f_{LO} + f_0|$, with f_0 denoting the interrogating frequency.

The response takes the $^{-1}$ position. Being separated from the interrogation by Δf, it falls inside the antenna bandwidth. A bandpass characteristic corresponding to a general drain/source loading circuit has been also added to this diagram.

Substituting the transistor in Fig. 1 by its nonlinear equivalent model, see [14], a time-varying circuit analysis of the mixer schematic may be made. Using the conversion matrix technique in [14], the spectral components of the device main nonlinearity, I^n_{ds}, may be related to the spectral components of its control voltages, V^n_{gs} and V^n_{ds},

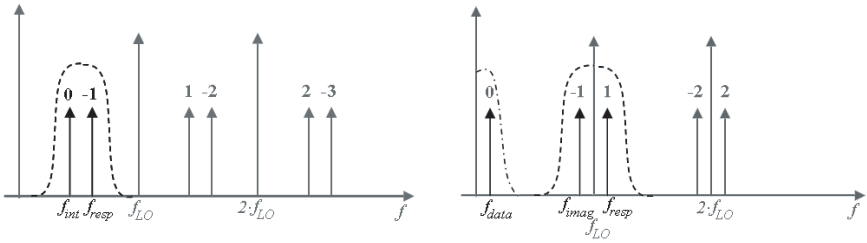

Figure 2. Spectral diagrams for the (a) resistive and (b) drain/source mixing modes. (- -) represents the bandpass response of the circuit at drain/source side, while (-.-) reproduces the lowpass gate circuit characteristic.

through the Fourier-series expansion coefficients, G_m^n and G_{ds}^n, of the periodic time-varying first order derivatives, $G_m(t)_{LO}$ and $G_{ds}(t)_{LO}$.

$$\begin{bmatrix} I_{ds}^{-N^*} \\ . \\ I_{ds}^{-1^*} \\ I_{ds}^{0} \\ I_{ds}^{1} \\ . \\ I_{ds}^{N} \end{bmatrix} = \begin{bmatrix} G_m^0 & . & G_m^{-N+1} & G_m^{-N} & G_m^{-N-1} & . & G_m^{-2N} \\ . & G_m^0 & . & . & . & . & . \\ G_m^{N-1} & . & G_m^0 & . & . & . & G_m^{-N-1} \\ G_m^N & . & G_m^1 & G_m^0 & G_m^{-1} & . & G_m^{-N} \\ G_m^{N+1} & . & . & . & G_m^0 & . & G_m^{-N+1} \\ . & . & . & . & . & G_m^0 & . \\ G_m^{2N} & . & G_m^{N+1} & G_m^N & G_m^{N-1} & . & G_m^0 \end{bmatrix} \cdot \begin{bmatrix} V_{gs}^{-N^*} \\ . \\ V_{gs}^{-1^*} \\ V_{gs}^{0} \\ V_{gs}^{1} \\ . \\ V_{gs}^{N} \end{bmatrix}$$

$$+ \begin{bmatrix} G_{ds}^0 & . & G_{ds}^{-N+1} & G_{ds}^{-N} & G_{ds}^{-N-1} & . & G_{ds}^{-2N} \\ . & G_{ds}^0 & . & . & . & . & . \\ G_{ds}^{N-1} & . & G_{ds}^0 & . & . & . & G_{ds}^{-N-1} \\ G_{ds}^N & . & G_{ds}^1 & G_{ds}^0 & G_{ds}^{-1} & . & G_{ds}^{-N} \\ G_{ds}^{N+1} & . & . & . & G_{ds}^0 & . & G_{ds}^{-N+1} \\ . & . & . & . & . & G_{ds}^0 & . \\ G_{ds}^{2N} & . & G_{ds}^{N+1} & G_{ds}^N & G_{ds}^{N-1} & . & G_{ds}^0 \end{bmatrix} \cdot \begin{bmatrix} V_{ds}^{-N^*} \\ . \\ V_{ds}^{-1^*} \\ V_{ds}^{0} \\ V_{ds}^{1} \\ . \\ V_{ds}^{N} \end{bmatrix} \quad (1)$$

Taking into account the resistive mode mixing conditions, see Fig. 2(a), the I_{ds} spectral components appearing at the response and interrogating frequencies can be reduced to:

$$\begin{bmatrix} I_{ds}^{-1^*} \\ I_{ds}^{0} \end{bmatrix} \approx \begin{bmatrix} G_{ds}^0 & G_{ds}^{-1} \\ G_{ds}^1 & G_{ds}^0 \end{bmatrix} \cdot \begin{bmatrix} V_{ds}^{-1^*} \\ V_{ds}^{0} \end{bmatrix} \quad (2)$$

where the V_{gs}^n mixing terms have been eliminated due to the fact that $G_m(t)_{LO}$ keeps null in cold operation. With the help of the drain/source side circuit load conditions at the interrogating and

response frequencies,

$$V_{ds}^{-1^*} = -I_{ds}^{-1^*} \cdot (R_d + R_s + Z_D) \tag{3a}$$

$$V_{ds}^{0} = V_{int} - I_{ds}^{0} \cdot (R_d + R_s + Z_D) \tag{3b}$$

with R_d and R_s representing the parasitic drain and source resistances, a simplified closed expression for the conversion gain may be obtained as

$$CG \approx \frac{4 \cdot \left|G_{ds}^{1}\right|^2 \cdot \mathrm{Real}^2\left\{Z_D\right\}}{\left|\left[1+G_{ds}^{0}\cdot(R_d+R_s+Z_D)\right]^2 - \left[G_{ds}^{1}\cdot(R_d+R_s+Z_D)\right]^2\right|^2} \tag{4}$$

It should be noticed that the influence of the reactive elements in the device equivalent circuit have been neglected, particularly because they have secondary influence on the mixer behavior dependence on LO level and bias voltage. In Fig. 3(a), this expression has been evaluated in terms of the LO power level and the V_{gs} DC bias for a conveniently characterized ATF54143 E-PHEMT from Avago. A minimum conversion loss, associated to a maximum $|G_{ds}^{1}|$, is predicted at the threshold position ($V_{GS} = 0.35\,\mathrm{V}$) for low LO power levels. This minimum gets wider and is shifted to the left of the V_{GS} axis with P_{LO}. For a LO excitation around 4 dBm, the operation with $V_{GS} = 0\,\mathrm{V}$ and $V_{DS} = 0\,\mathrm{V}$ is close to the optimum.

2.3. Drain/Source Mixing Mode for RFID Operation

In the second operating mode, a low frequency data signal applied at gate port, $VG = V_{data}$, is up-converted by means of a time varying transconductance, thanks to the injection of a LO interrogating signal

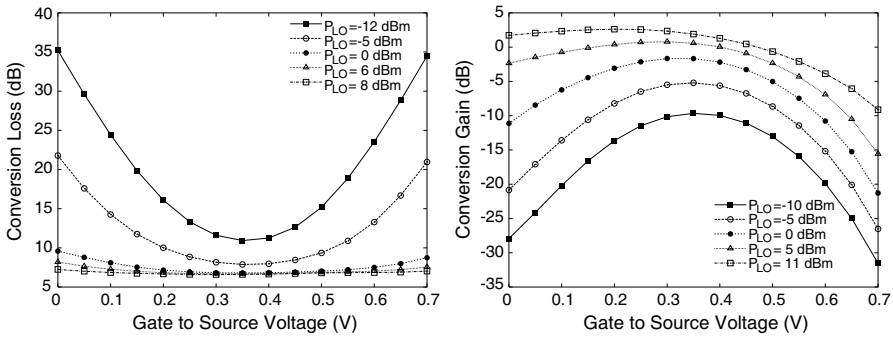

Figure 3. Predicted conversion behavior: (a) Resistive and (b) active mixing modes.

by drain/source side. This kind of operation would represent the classic RFID single tag operation. Taking this into account, a simplified spectral diagram has been also represented in Fig. 2(b).

The response takes the ^{1} position, with f_0 denoting in this case the data frequency. The $^{-1}$ Dirac delta represents the image signal, falling in this case inside the drain/source circuit bandpass response (usually imposed by the antenna). This has been depicted in Fig. 2(b) together with the frequency characteristic of a lowpass gate circuit. The I_{ds} mixing components appearing at the response and image frequencies can be approximated in this case by:

$$\begin{bmatrix} I_{ds}^{-1^*} \\ I_{ds}^{1} \end{bmatrix} \approx \begin{bmatrix} G_m^{-1} \\ G_m^{1} \end{bmatrix} \cdot V_{gs}^{0} + \begin{bmatrix} G_m^{0}/2 + G_{ds}^{0} & G_m^{-2}/2 + G_{ds}^{-2} \\ G_m^{2}/2 + G_{ds}^{2} & G_m^{0}/2 + G_{ds}^{0} \end{bmatrix} \cdot \begin{bmatrix} V_{ds}^{-1^*} \\ V_{ds}^{1} \end{bmatrix} \quad (5)$$

Introducing the load conditions at both sides,

$$V_{gs}^{0} \approx V_{data} \quad (6a)$$

$$V_{ds}^{1} = -I_{ds}^{1} \cdot (R_d + R_s + Z_D) \quad (6b)$$

$$V_{ds}^{-1^*} = -I_{ds}^{-1^*} \cdot (R_d + R_s + Z_D) \quad (6c)$$

it takes us to a simplified conversion gain expression:

$$CG = \frac{4 \cdot \left|G_m^{1}\right|^2 \cdot \left|1 + \left(\tilde{G}_{ds}^{0} - \tilde{G}_{ds}^{2}\right) \cdot (R_d + R_s + Z_D)\right|^2 \cdot \mathrm{Real}\{Z_D\} \cdot \mathrm{Real}\{Z_G\}}{\left|\left[1 + \tilde{G}_{ds}^{0} \cdot (R_d + R_s + Z_D)\right]^2 - \left[\tilde{G}_{ds}^{2} \cdot (R_d + R_s + Z_D)\right]^2\right|^2} \quad (7a)$$

$$\tilde{G}_{ds}^{0} \approx G_m^{0}/2 + G_{ds}^{0} \quad (7b)$$

$$\tilde{G}_{ds}^{2} \approx G_m^{2}/2 + G_{ds}^{2} \quad (7c)$$

The evaluation of this expression is presented in Fig. 3(b). It can also be noticed that a small gain conversion is possible, appearing at the device threshold value for low power levels, and experimenting a change with P_{LO} and V_{GS} analogous to the resistive mixer case. Optimum operation at $V_{GS} = 0\,\mathrm{V}$ seems to be perfectly possible, although higher LO levels are required (around 11 dBm), as expected [10]. Although operation without gate and drain biasing voltages is perfectly possible, the "active" adjective is kept to describe a mixing mode based on a time-varying transconductance. Gain conversion without DC bias is possible, at the expense of an adequate LO power level.

These results have theoretically shown the possibility of using a common E-PHEMT topology for two different mixing modes without the need for DC bias.

2.4. Implemented Mixer Characterization

In Fig. 4, a view of a hybrid implementation of the dual-mode mixer is presented. A lumped element diplexer was added at gate side for properly applying a LO excitation or a data signal to that terminal, according to the mode. For the balun, a commercial Anaren part (3A425) has been used.

The possibility of applying a gate DC voltage was included for characterizing the mixer behavior evolution with both the LO power level and V_{GS} DC bias. In the resistive mode, a 890 MHz interrogating signal ($P_{RF} = -15$ dBm) was applied from drain/source side, while the response signal (910 MHz) was extracted from the same side using a directional coupler. The LO frequency was set to 1800 MHz. For the drain/source mixer case, a 890 MHz LO signal was used to up-convert a 55 MHz data signal applied at gate terminal (half the bandwidth of the antenna to be introduced in next section).

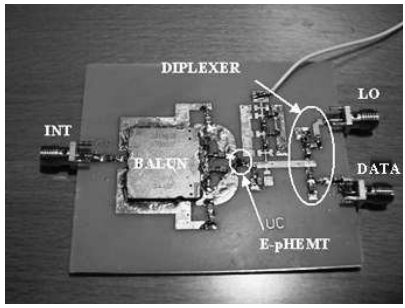

Figure 4. Photograph of the lab dual-mode mixer model.

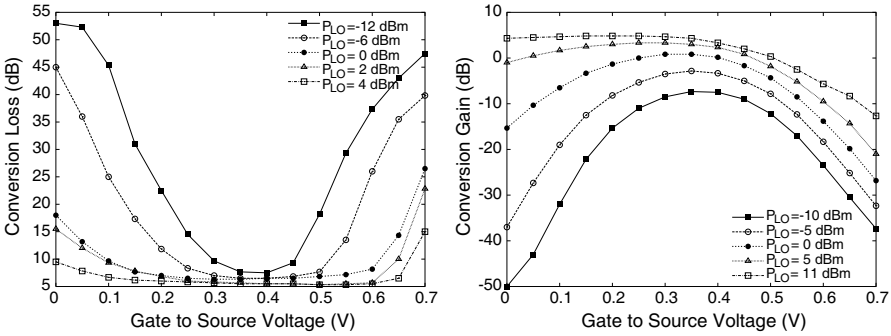

Figure 5. Measured conversion behavior: (a) Resistive and (b) active mixing mode.

In Fig. 5, measured results for the conversion efficiency are plotted.

When compared to Fig. 3 and despite the assumed simplifications, the predictions from (4) and (7) are very good. Both sets of curves validate our proposed approach for introducing E-PHEMT devices in unbiased frequency translating functions for multimode wireless transponders.

In order to reduce circuit sensitivity to the variation of device parameters with ageing, temperature or process, an adequate resistor may be added in the gate biasing (DC) path. Taking advantage of the existence of a small gate current value at the selected operating conditions, the resistor introduces a gate to source voltage correction mechanism, able of minimizing the impact of the above mentioned phenomena over the circuit performance, while also improving long term reliability.

3. ACTIVE ANTENNA

In the search for low cost, compact and functional radiating solutions, active antennas have emerged as promising candidates. These reasons have led to implement the proposed dual-mode mixing technique employing active antenna concepts.

3.1. Antenna Element

In [15], a dual feed printed structure was suggested for implementing a two-device singly balanced resistive mixer. A similar idea was here applied to avoid the use of the balun circuit in the proposed mixer.

An square aperture-coupled patch [16–19] with opposite side excitation of the same TM_{10} mode was designed and constructed at the 900 MHz band. This kind of radiator provides an acceptable bandwidth and is suitable for active circuit integration. The dimensions were first selected to assure $50\,\Omega$ matching conditions. However, in the search for improving the antenna dual-mode conversion figures further refinements were performed trying to assure a better match to the input/output mixer equivalent circuits. The dimensions of the optimized antenna can be seen in Fig. 6(a). A high permitivity thin substrate can be employed for the circuit elements and feed lines, in this case 30mils N25 substrate from Arlon, while air substrate [20] can be used for the antenna. Fig. 6(b) shows the simulated and measured input matching and isolation between the antenna ports. As can be seen, with this type of feeding a sort of spatial power combining is guaranteed but with a poor isolation between the ports.

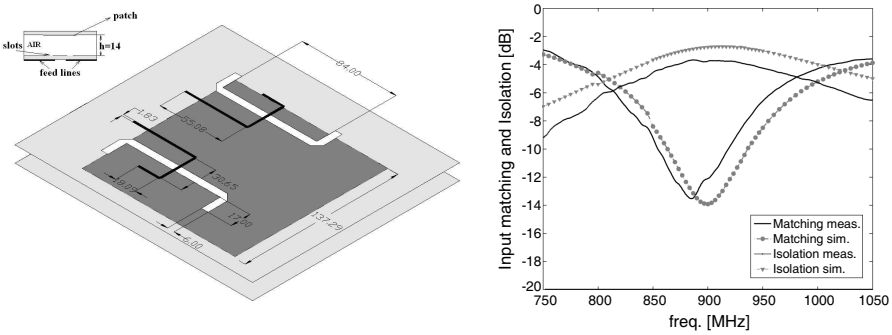

Figure 6. (a) Top and side views of the designed patch. Dimensions in mm. (b) Simulated and measured input matching and isolation between the antenna ports.

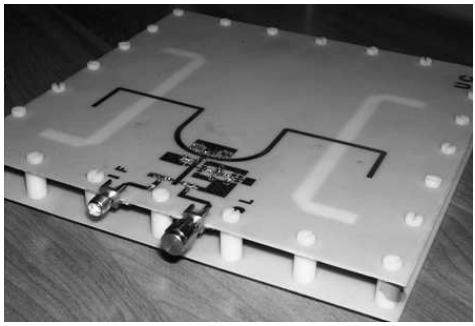

Figure 7. Implemented active mixing antenna.

The antenna presents a quite good efficiency along the operating frequency band, higher than 90% in the vicinity of the resonance frequency (900 MHz) although at the high end of the band (950 MHz) is degraded up to 81%. The measured gain (dBi) presents a deviation of less than 1 dB in the desired bandwidth, whereas the beamwidth is maintained practically constant in the whole frequency band.

3.2. Measurement Results

For appropriate characterizing this structure, the test set-up of Fig. 8 was employed [19, 21]. A 890 MHz signal was transmitted using a high directivity antenna, and the response power level received back from the transponder was measured.

For the phase conjugator case, a 1800 MHz LO signal was applied through the highpass path of the gate diplexer, and the 910 MHz response signal was characterized versus elevation at $V_{GS} = 0$ V and $P_{LO} = 4$ dBm. For the classic RFID tag case, the same interrogation was used, but with a much higher power level. A 55 MHz excitation was

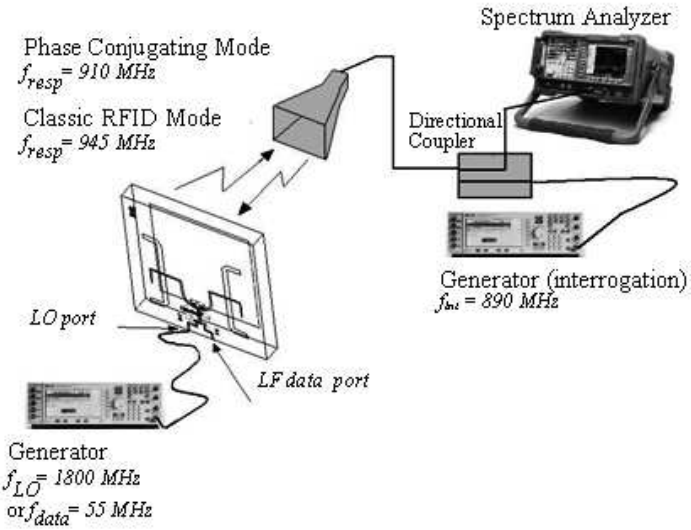

Figure 8. Employed test set-up.

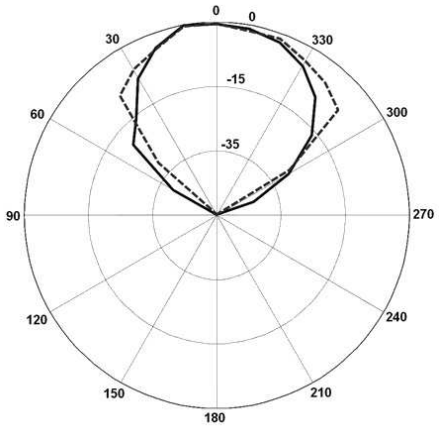

Figure 9. Normalized received power response versus elevation: (——) phase conjugator, and (- - -) classic RFID tag mode.

applied to the lowpass diplexer path, and the 945 MHz response signal was characterized with the elevation angle. The normalized radiation patterns are shown in Fig. 9.

The received power evolution for the phase conjugating mode corresponds to the dual-feed patch radiation diagram, independently of the interrogating power level. In the classic RFID tag response or lecture mode, the power evolution nearly follows the patch diagram for high LO transmitted levels (the case represented in Fig. 9). For lower values, the measured characteristic may deviate from that behavior due to the strong dependence of conversion gain with LO power, as observed in Figs. 3(b) and 5(b).

4. CONCLUSIONS

A zero-bias dual-mode mixer has been proposed in this paper for its use as transponder on wireless identification/communication applications. Simple closed form expressions for the conversion gain have been obtained through a time-varying circuit analysis. A lab model has been designed and tested, being a 7 dB conversion loss obtained for the resistive mode while a 3.83 dB gain measured in the drain/source active operation. Finally, a time-varying compact active antenna has been developed and tested with success for two different transponder scenarios: classic coded response and phase conjugated retransmission. The same transponder could be employed as individual sensor tag, or as integrated element of a retrodirective sensor network base station.

ACKNOWLEDGMENT

This work was supported by Ministerio de Ciencia e Innovación through projects TEC2008-06684-C03-01 and CSD2008-00068. The authors also thank the support provided by AECID through action D/018607/08.

REFERENCES

1. Loo, C.-H., K. Elmahgoub, F. Yang, A. Z. Elsherbeni, D. Kajfez, A. A. Kishk, T. Elsherbeni, L. Ukkonen, L. Sydanheimo, M. Kivikoski, S. Merilampi, and P. Ruuskanen, "Chip impedance matching for UHF RFID tag antenna design," *Progress In Electromagnetics Research*, PIER 81, 359–370, 2008.
2. "An automatic vehicle ID system for toll collecting," Lawrence Livermore Nat. Lab., Rep. No. UCRL-TB-113409, Apr. 1993.

3. Ohta, T., H. Nakano, and M. Tokuda, "Compact microwave remote recognition system with newly developed SSB modulation," *1990 IEEE MTT-S Int. Microwave Symp. Dig.*, 957–960, Dallas, USA, Jun. 1990.
4. Kim, D.-Y., H.-G. Yoon, B.-J. Jang, and J.-G. Yook, "Interference analysis of UHF RFID systems," *Progress In Electromagnetics Research B*, Vol. 4, 115–126, 2008.
5. Page, R., "A low power RF ID transponder," *RF Design*, 31–36, Jul. 1993.
6. Pobanz, C. W. and T. Itoh, "A microwave noncontact identification transponder using subharmonic-interrogation," *IEEE Trans. Microwave Theory and Tech.*, Vol. 43, No. 7, 1673–1679, Jul. 1995.
7. Miyamoto, R. Y. and T. Itoh, "Retrodirective arrays for wireless communications," *IEEE Microwave Magazine*, Vol. 3, No. 1, 71–79, Mar. 2002.
8. Guo, Y.-C., X.-W. Shi, and L. Chen, "Retrodirective array technology," *Progress In Electromagnetics Research B*, Vol. 5, 153–167, 2008.
9. Pon, C. Y., "Retrodirective array using the heterodyne technique," *IEEE Trans. Antennas Propagat.*, Vol. 12, 176–180, Dec. 1964.
10. Maas, S. A., *The RF and Microwave Circuit Design Cookbook*, Artech House, Boston, 1998.
11. Yhland, K., N. Rorsman, and H. H. G. Zirath, "Novel single device balanced resistive HEMT mixer," *IEEE Trans. Microwave Theory and Tech.*, Vol. 43, No. 12, 2863–2867, Dec. 1995.
12. García, J. A., E. Malaver, and L. Cabria, "A zero-bias single-device balanced E-PHEMT mixer with conversion gain for RFID applications," *2003 IEEE MTT-S Int. Microwave Symp. Dig.*, 1311-1314, Philadelphia, USA, Jun. 2003.
13. Yhland, K., "Resistive FET mixers," Ph. D. dissertation, Dept. Microelectronics ED, Chalmers University of Technology at Göteborg, Sweden, 1999.
14. Maas, S. A., *Nonlinear Microwave Circuits, Butler.*, Artech House, Norwood, MA, 1988.
15. Pobanz, C. W., "Time-varying active antennas: Circuits and applications," Ph. D. dissertation, University of California, Los Angeles, 1997.
16. Pozar, D. M., "A microstrip antenna aperture coupled to a microstrip line," *Electronics Lett.*, Vol. 21, 49–50, Jan. 1985.
17. Ghassemi, N., J. Rashed-Mohassel, M. H. Neshati, S. Tavakoli,

and M. Ghassemi, "A high gain dual stacked aperture coupled microstrip antenna for wideband applications," *Progress In Electromagnetics Research B*, Vol. 9, 127–135, 2008.

18. Zhang, M., Y. Chen, Y. Jiao, and F. Zhang, "Dual circularly polarized antenna of compact structure for RFID application," *Journal of Electromagnetic Waves and Applications*, Vol. 20, No. 14, 1895–1902, 2006.
19. Vázquez, C., S. ver Hoeye, G. León, M. Fernández, L. F. Herrán, and F. Las Heras, "Transmitting polarisation agile microstrip antenna based on injection locked oscillators," *Journal of Electromagnetic Waves and Applications*, Vol. 22, No. 17–18, 2427–2437, 2008.
20. Ayoub, A. F. A., "Analysis of rectangular microstrip antennaswith air substrates," *Journal of Electromagnetic Waves and Applications*, Vol. 17, No. 12, 1755–1766, Dec. 2003.
21. Chou, H. T., L. R. Kuo, and W. J. Liao, "Characteristic evaluation of an active patch antenna structure with an embedded lna module for GPS reception," *Journal of Electromagnetic Waves and Applications*, Vol. 21, No. 5, 599–614, 2007.